



**HAL**  
open science

## Unexpected winter phytoplankton blooms in the North Atlantic subpolar gyre

L. Lacour, M. Ardyna, K. F Stec, H. Claustre, L. Prieur, A. Poteau, M Ribera d'Alcala, D. Iudicone

► **To cite this version:**

L. Lacour, M. Ardyna, K. F Stec, H. Claustre, L. Prieur, et al.. Unexpected winter phytoplankton blooms in the North Atlantic subpolar gyre. *Nature Geoscience*, 2017, 10 (11), pp.836-839. 10.1038/ngeo3035 . hal-03515671

**HAL Id: hal-03515671**

**<https://hal.science/hal-03515671>**

Submitted on 6 Jan 2022

**HAL** is a multi-disciplinary open access archive for the deposit and dissemination of scientific research documents, whether they are published or not. The documents may come from teaching and research institutions in France or abroad, or from public or private research centers.

L'archive ouverte pluridisciplinaire **HAL**, est destinée au dépôt et à la diffusion de documents scientifiques de niveau recherche, publiés ou non, émanant des établissements d'enseignement et de recherche français ou étrangers, des laboratoires publics ou privés.

# 1 **Unexpected winter phytoplankton blooms in the North Atlantic Subpolar Gyre**

2 **Authors:** L. Lacour<sup>1\*</sup>, M. Ardyna<sup>1</sup>, K. F. Stec<sup>2</sup>, H. Claustre<sup>1</sup>, L. Prieur<sup>1</sup>, A. Poteau<sup>1</sup>, M. Ribera  
3 D'Alcala<sup>2</sup>, D. Iudicone<sup>2</sup>

4 \*Correspondence to: leo.lacour@obs-vlfr.fr.

## 6 **Affiliations:**

7 <sup>1</sup>Sorbonne Universités, UPMC Univ Paris 06, CNRS, Laboratoire d'Océanographie de  
8 Villefranche (LOV), Observatoire Océanologique, 06230 Villefranche-sur-Mer, France

9 <sup>2</sup>Laboratory of Ecology and Evolution of Plankton, Stazione Zoologica Anton Dohrn, Naples,  
10 Italy

11  
12 **Introductory paragraph: In mid- and high-latitude oceans, winter surface cooling and**  
13 **strong winds drive turbulent mixing that carries phytoplankton to depth of several**  
14 **hundred meters, well below the sunlit layer. This downward mixing, in combination with**  
15 **low solar radiation, drastically limits phytoplankton growth during the winter, especially**  
16 **that of the diatoms and other species that are involved in seeding the spring bloom. Here**  
17 **we present observational evidence for widespread winter phytoplankton blooms in a large**  
18 **part of the North Atlantic Subpolar Gyre from autonomous profiling floats equipped with**  
19 **biogeochemical sensors. These blooms were triggered by intermittent restratification of**  
20 **the mixed layer when mixed layer eddies led to a horizontal transport of lighter water**  
21 **over denser layers. Combining a bio-optical index with complementary chemotaxonomic**  
22 **and modelling approaches, we show that these restratification events increase**  
23 **phytoplankton residence time in the sunlight zone, resulting in greater light interception**

24 **and the emergence of winter blooms. Restratification also caused a phytoplankton**  
25 **community shift from pico- and nanophytoplankton to phototrophic diatoms. We**  
26 **conclude that transient winter blooms can maintain active diatom populations throughout**  
27 **the winter months, directly seeding the spring bloom and potentially making a significant**  
28 **contribution to over-winter carbon export.**

29

30 The Sverdrup paradigm <sup>1</sup> postulates that deep winter mixing prevents phytoplankton biomass  
31 accumulation since losses exceed light-limited production. However, few wintertime in situ  
32 observations revealed significant phytoplankton stock in deep mixed layers <sup>2,3</sup>. Based on  
33 modelling simulations, orbital motions triggered by deep convection have been suggested to  
34 allow recurrent incursions of phytoplankton to the surface lit layer, and thus supporting a winter  
35 production <sup>4</sup>. Furthermore, winter deepening of the mixed layer would dilute plankton  
36 concentration, thus reducing grazing pressure, and consequently, phytoplankton loss  
37 (disturbance-recovery hypothesis) <sup>5,6</sup>. Despite low phytoplankton growth, biomass may  
38 accumulate throughout winter in deep mixed layers.

39 Modelling studies have shown that mixed layer eddies (MLEs) growing from horizontal  
40 density gradients can generate vertical restratification of the mixed layer at spatial scales of 1-  
41 10 km and time scales of days <sup>7,8</sup>, thus allowing patchy blooms to be initiated before the vernal  
42 stratification <sup>9</sup>. MLEs being potentially much more frequent in winter <sup>10</sup>, such restratification  
43 mechanism may provide an additional mechanism for winter phytoplankton growth.

44 In addition, other studies have proposed that a reduction in turbulent mixing, due to a  
45 relaxation in atmospheric forcing, may allow phytoplankton to grow, before the vernal  
46 restratification (critical turbulence hypothesis) <sup>11-13</sup>.

47 In this context, distinguishing the mixing layer depth from the mixed layer depth is  
48 important when dealing with phytoplankton dynamics<sup>14-16</sup>. In the following, we improved the  
49 determination of the mixed layer depth to be the closest to the mixing layer depth (see  
50 Supplementary Methods 1.4) given that there are no large scale, autonomous measurements of  
51 turbulence so far.

## 52 **Winter mixing intermittency**

53 The common view is that the North Atlantic subpolar ocean is continuously deeply  
54 mixed during winter<sup>17,18</sup>. However, around 25% of Argo density profiles in this area were  
55 stratified (mixed layer depth (MLD) < 100 m, Supplementary Methods 1.4) during the winters  
56 of 2014 and 2015 (Fig. 1a and Supplementary Fig. 4). The vertical stratification was particularly  
57 strong in areas of significant horizontal density gradients (Fig. 1b), suggesting the potential role  
58 of MLEs. MLEs drive net horizontal transfer of lighter water above heavier water that can  
59 locally stratify the mixed layer. Similar temperature and salinity structure (i.e. Turner angle<sup>19</sup>)  
60 between horizontal and vertical density gradients in the subpolar gyre (Fig. 1c, Supplementary  
61 Methods 1.3) confirm the crucial role of lateral processes in restratifying the deep winter mixed  
62 layer in the North Atlantic Subpolar Gyre.

63 Restratification mechanisms compete with vertical mixing induced mainly by surface  
64 wind and cooling<sup>9</sup>. Thus, restratification events require sufficiently long calm periods with a  
65 relaxation of this atmospheric forcing. While analysing wind speed and heat fluxes, we  
66 observed that some regions of the subpolar gyre presented up to 30% of calm periods (Fig. 1d,  
67 Supplementary Fig. 5 and Methods 1.6). A proxy of the sea state (i.e. wave height,  
68 Supplementary Methods 1.7), derived from BGC-Argo floats, also confirmed evidence of calm  
69 periods (i.e. 20% of the winter profiles, Supplementary Fig. 7). Therefore, transient calm  
70 periods appear to be frequent across the North Atlantic Subpolar Gyre, allowing restratification  
71 to be a recurrent feature in winter.

72

### 73 **Mixing intermittency triggers winter phytoplankton blooms**

74        Restratification events triggered winter phytoplankton accumulations in the surface  
75 layer in the whole subpolar gyre (based on two different proxies of phytoplankton biomass:  
76 chlorophyll *a* (chl<sub>a</sub>) and particulate optical backscattering (b<sub>bp</sub>); Fig. 2 and Supplementary Fig.  
77 9). These restratification events maintain phytoplankton cells in the euphotic zone (surface to  
78 Z<sub>e</sub>; see Fig. 2b and Supplementary Fig. 15), enhancing the light availability for their growth.  
79 Indeed, the light level (i.e. the daily-integrated Photosynthetically Available Radiation (PAR)  
80 averaged over the MLD) increased ten-fold in average in stratified conditions (MLD < 100 m;  
81 1.3 mol photons m<sup>-2</sup>) compared to deeply mixed conditions (MLD > 100 m; 0.13 mol photons  
82 m<sup>-2</sup>). For 70% of the stratified profiles (Fig. 2b, top panel), an increase in light exposure led to  
83 the occurrence of winter blooms, defined here as a biomass increase of 5% above the winter  
84 median value (75% of the stratified profiles using b<sub>bp</sub> instead of chl<sub>a</sub>). These observations  
85 suggest that most of the calm periods lasted long enough to initiate locally transient winter  
86 phytoplankton blooms.

87        Importantly, distinct light environments between stratified and deeply mixed conditions  
88 impacted not only phytoplankton production but also the structure of the community<sup>20,21</sup>. An  
89 optical community index (chl<sub>a</sub> to b<sub>bp</sub> ratio<sup>22</sup>) derived from BGC-Argo float measurements,  
90 revealed a clear shift in the phytoplankton community structure during restratification events.  
91 In typical winter conditions (i.e., deep mixed layers with low surface daily-integrated PAR),  
92 pico- and nanophytoplankton clearly dominated the overall phytoplankton community in the  
93 subpolar gyre (Fig. 3a). By contrast, the proportion of diatoms temporarily increases during  
94 transient restratification events when their growth was evidently boosted by more favourable  
95 light conditions (Fig. 3a, b). These blooms became particularly frequent in late February and  
96 March (10-25% of the all profiles, n = 30, Fig. 3b), when frequency of restratification events

97 increased (20-40% of the all profiles,  $n = 86$ ;  $r = 0.94$ ,  $p$ -value  $< 0.01$ ) and surface daily-  
98 integrated PAR was higher due to longer daylength (Fig. 3c). Variation of the cloudiness (dot  
99 size in Fig. 3c) also reinforced the critical role of light level, and its impact on changing the  
100 community composition in winter. During calm periods with clear sky conditions, higher  
101 surface daily-integrated PAR significantly boosted the growth of diatoms (Fig. 3c;  $r = 0.56$ ,  $p$ -  
102 value  $< 0.01$ , see supplementary Table.3). These findings have been corroborated by rare  
103 phytoplankton pigment samples collected during a winter cruise in the Newfoundland Basin  
104 (CATCH, January-February 1997, Fig. 2a and Supplementary Methods 1.10 and 2.5). While  
105 deep mixing layers were dominated by chryso- and pelagophytes, contributing to almost 50%  
106 of the total chl $a$ , diatoms became a relevant group contributing to almost 20% of the total chl $a$   
107 when MLD shoaled above 100 m (Supplementary Fig. 16).

108

### 109 **Reassessing the winter as an active phytoplankton period**

110 Moderate to high light-adapted diatoms thriving in spring are not likely able to survive  
111 in deep winter mixed layers. A set of suitable overwintering strategies, e.g. formation of resting  
112 cells or spores<sup>23,24</sup>, have been highlighted as means to survive harsh winter conditions. Here,  
113 we show that diatoms can remain physiologically active throughout winter by benefiting from  
114 transient restratification events and thus more favourable light environments (Supplementary  
115 Fig. 17 and 19). By contrast, the persistence of pico- and nanophytoplankton, especially small  
116 flagellates, and their dominance in deep mixing layers may be explained by mixotrophy, the  
117 combined use of phototrophy and heterotrophy within a single organism<sup>25</sup>. The shift to  
118 heterotrophy during long period of darkness at depth could confer to these organisms a serious  
119 ecological advantage and bring an alternative hypothesis to the disturbance-recovery hypothesis  
120 <sup>5</sup>.

121 An extraordinary number of studies emerged during the last decade to understand the  
122 dynamics of the high-latitude spring bloom (i.e. timing and magnitude). However, the vigorous  
123 debate on spring bloom dynamics has remained mainly focused on physical controls of  
124 phytoplankton biomass accumulation. Our observations reveal that the physical environment  
125 plays a key role also in shaping the community structure during the preconditioning period of  
126 the spring bloom. Although transient winter blooms, supported by mixing intermittency, are  
127 not intense in term of biomass, they maintain an active diatom population throughout winter.  
128 Unlike resting cells or spores that require a germination period <sup>26</sup>, active winter diatoms can  
129 directly seed the spring bloom, hence impacting the bloom timing and potentially its magnitude.

130

### 131 **Implications for spring bloom and carbon export dynamics**

132 Results of a parallel subpolar phytoplankton community model (Supplementary  
133 Methods 2.7) support the claim that intermittent winter stratification can affect spring bloom  
134 characteristics. Restratification events in winter boost diatom net growth rate (Supplementary  
135 Fig. 17), increasing the standing stock of diatoms towards spring. Mixing intermittency may  
136 increase by up to 2 fold the bloom magnitude and bring the bloom peak timing forward by up  
137 to 19 days (Supplementary Fig. 19 and Table 7). These results not only corroborate in situ  
138 observations (i.e. BGC-Argo and CATCH data) but further suggest a possible impact of winter  
139 mixing intermittency on the observed yet unexplained <sup>27</sup> interannual variability of spring  
140 blooms.

141 Unexpected wintertime occurrence of diatom blooms in the subpolar gyre could also  
142 challenge our perception of the spring bloom-dependent carbon export. Alternation of  
143 stratification and deep mixing allows transient diatom blooms along with non-sinking particles  
144 and dissolved organic and inorganic carbon to be transferred rapidly to depth (the so-called

145 mixed layer pump<sup>28–30</sup>). Even though a single event transfers only a low carbon stock compared  
146 to the spring bloom, cumulative events over the winter months may contribute significantly to  
147 the annual carbon export.

148

## 149 **Methods**

150 Methods and supplementary figures are available in the supplementary information.

### 151 Data availability

152 Argo data were collected and made freely available by the International Argo Program and the  
153 CORIOLIS project that contribute to it (<http://www.coriolis.eu.org>). BGC-Argo data are  
154 publicly available at <ftp://ftp.ifremer.fr/ifremer/argo/dac/coriolis/>. Net heat flux and wind data  
155 were extracted from the ECMWF ERA Interim dataset (reanalysis) freely available at  
156 <http://apps.ecmwf.int/datasets/data/interim-full-daily/levtype=sfc>. The MLD climatology was  
157 provided by Ifremer (<http://www.ifremer.fr/cerweb/deboyer/mld/home.php>).

158

## 159 **References**

- 160 1. Sverdrup, H. U. On conditions for the vernal blooming of phytoplankton. *J. du Cons.*  
161 *Int. pour l'exploitation la mer* **18**, 287–295 (1953).
- 162 2. Backhaus, J. O. *et al.* Convection and primary production in winter. *Mar. Ecol. Progr.*  
163 *Ser.* **251**, 1–14 (2003).
- 164 3. Dale, T., Rey, F. & Heimdal, B. R. Seasonal development of phytoplankton at a high  
165 latitude oceanic site. *Sarsia* **84**, 419–435 (1999).
- 166 4. Große, F., Lindemann, C., Pätsch, J. & Backhaus, J. O. The influence of winter

- 167 convection on primary production: A parameterisation using a hydrostatic three-  
168 dimensional biogeochemical model. *J. Mar. Syst.* **147**, 138–152 (2015).
- 169 5. Behrenfeld, M. J. Abandoning Sverdrup’s Critical Depth Hypothesis on phytoplankton  
170 blooms. *Ecology* **91**, 977–989 (2010).
- 171 6. Behrenfeld, M. J., Doney, S. C., Lima, I., Boss, E. S. & Siegel, D. A. Annual cycles of  
172 ecological disturbance and recovery underlying the subarctic Atlantic spring plankton  
173 bloom. *Global Biogeochem. Cycles* **27**, 526–540 (2013).
- 174 7. Boccaletti, G., Ferrari, R. & Fox-Kemper, B. Mixed Layer Instabilities and  
175 Restratification. *J. Phys. Oceanogr.* **37**, 2228–2250 (2007).
- 176 8. Fox-Kemper, B., Ferrari, R. & Hallberg, R. Parameterization of Mixed Layer Eddies.  
177 Part I: Theory and Diagnosis. *J. Phys. Oceanogr.* **38**, 1145–1165 (2008).
- 178 9. Mahadevan, a., D’Asaro, E., Lee, C. & Perry, M. J. Eddy-Driven Stratification  
179 Initiates North Atlantic Spring Phytoplankton Blooms. *Science (80-. )*. **337**, 54–58  
180 (2012).
- 181 10. Callies, J., Ferrari, R., Klymak, J. M. & Gula, J. Seasonality in submesoscale  
182 turbulence. *Nat. Commun.* **6**, 6862 (2015).
- 183 11. Huisman, J. & Weissing, F. J. Biodiversity of plankton by species oscillations and  
184 chaos. *Nature* **402**, 407–410 (1999).
- 185 12. Taylor, J. R. & Ferrari, R. Shutdown of turbulent convection as a new criterion for the  
186 onset of spring phytoplankton blooms. *Limnol. Ocean.* **56(6)**, 2293–2307 (2011).
- 187 13. Ferrari, R., Merrifield, S. T. & Taylor, J. R. Shutdown of convection triggers increase  
188 of surface chlorophyll. *J. Mar. Syst.* **147**, 116–122 (2015).

- 189 14. Brainerd, K. E. & Gregg, M. C. Surface mixed and mixing layer depths. *Deep. Res.*  
190 *Part I* **42**, 1521–1543 (1995).
- 191 15. Franks, P. J. S. Has Sverdrup’s critical depth hypothesis been tested? Mixed layers vs.  
192 turbulent layers. *ICES J. Mar. Sci.* **72**, 1897–1907 (2015).
- 193 16. Brody, S. R. & Lozier, M. S. Changes in dominant mixing length scales as a driver of  
194 subpolar phytoplankton bloom initiation in the North Atlantic. *Geophys. Res. Lett.* **41**,  
195 3197–3203 (2014).
- 196 17. Behrenfeld, M. J. & Boss, E. S. Resurrecting the ecological underpinnings of ocean  
197 plankton blooms. *Ann. Rev. Mar. Sci.* **6**, 167–194 (2014).
- 198 18. Lindemann, C. & St. John, M. A. A seasonal diary of phytoplankton in the North  
199 Atlantic. *Front. Mar. Sci.* **1**, 37 (2014).
- 200 19. Johnson, L., Lee, C. M. & D’Asaro, E. A. Global Estimates of Lateral Springtime  
201 Restratification. *J. Phys. Oceanogr.* **46**, 1555–1573 (2016).
- 202 20. Litchman, E. Growth rates of phytoplankton under fluctuating light. *Freshw. Biol.* **44**,  
203 223–235 (2000).
- 204 21. Walter, B., Peters, J., Van Beusekom, J. E. E. & St. John, M. A. Interactive effects of  
205 temperature and light during deep convection: A case study on growth and condition of  
206 the diatom *Thalassiosira weissflogii*. *ICES J. Mar. Sci.* **72**, 2061–2071 (2015).
- 207 22. Cetinić, I. *et al.* A simple optical index shows spatial and temporal heterogeneity in  
208 phytoplankton community composition during the 2008 North Atlantic Bloom  
209 Experiment. *Biogeosciences* **12**, 2179–2194 (2015).
- 210 23. Smetacek, V. S. Role of sinking in diatom life-history cycles: ecological, evolutionary  
211 and geological significance. *Mar. Biol.* **84**, 239–251 (1985).

- 212 24. McQuoid, M. R. & Hobson, L. A. Diatom resting stages. *J. Phycol.* **32**, 889–902  
213 (1996).
- 214 25. Caron, D. A. Mixotrophy stirs up our understanding of marine food webs. *Proc. Natl.*  
215 *Acad. Sci. U. S. A.* **113**, 2806–2808 (2016).
- 216 26. Smayda, T. J. & Mitchell-Innes, B. Dark survival of autotrophic, planktonic marine  
217 diatoms. *Mar. Biol.* **25**, 195–202 (1974).
- 218 27. Barton, A. D., Lozier, M. S. & Williams, R. G. Physical controls of variability in North  
219 Atlantic phytoplankton communities. *Limnol. Oceanogr.* **60**, 181–197 (2014).
- 220 28. Gardner, W. D., Chung, S. P., Richardson, M. J. & Walsh, I. D. The oceanic mixed-  
221 layer pump. *Deep Sea Res. Part II Top. Stud. Oceanogr.* **42**, 757–775 (1995).
- 222 29. Dall’Olmo, G. & Mork, K. A. Carbon export by small particles in the Norwegian Sea.  
223 *Geophys. Res. Lett.* **41**, 2921–2927 (2014).
- 224 30. Koeve, W., Pollehne, F., Oschlies, A. & Zeitzschel, B. Storm-induced convective  
225 export of organic matter during spring in the northeast Atlantic Ocean. *Deep. Res. Part*  
226 *I Oceanogr. Res. Pap.* **49**, 1431–1444 (2002).

227

## 228 **Corresponding author**

229 Correspondence and requests for materials should be addressed to L.L. (leo.lacour@obs-vlfr.fr)

230

## 231 **Acknowledgements**

232 We thank N. Briggs, M. J. Perry, E. D’Asaro, B. Gentili, E. Boss and F. Benedetti for fruitful  
233 discussions, C. Schmechtig for BGC-Argo float data management and Joséphine Ras for

234 proofreading the manuscript. We also thank Simon Wright for sharing the CHEMTAX software  
235 v.1.95, and Clément de Boyer Montégut for providing the MLD climatology. This work  
236 represents a contribution to the remOcean project (REMotely sensed biogeochemical cycles in  
237 the OCEAN, GA 246777) funded by the European Research Council, the ATLANTOS EU  
238 project (grant agreement 2014-633211) funded by H2020 program and the Italian Flagship  
239 Program RITMARE.

240

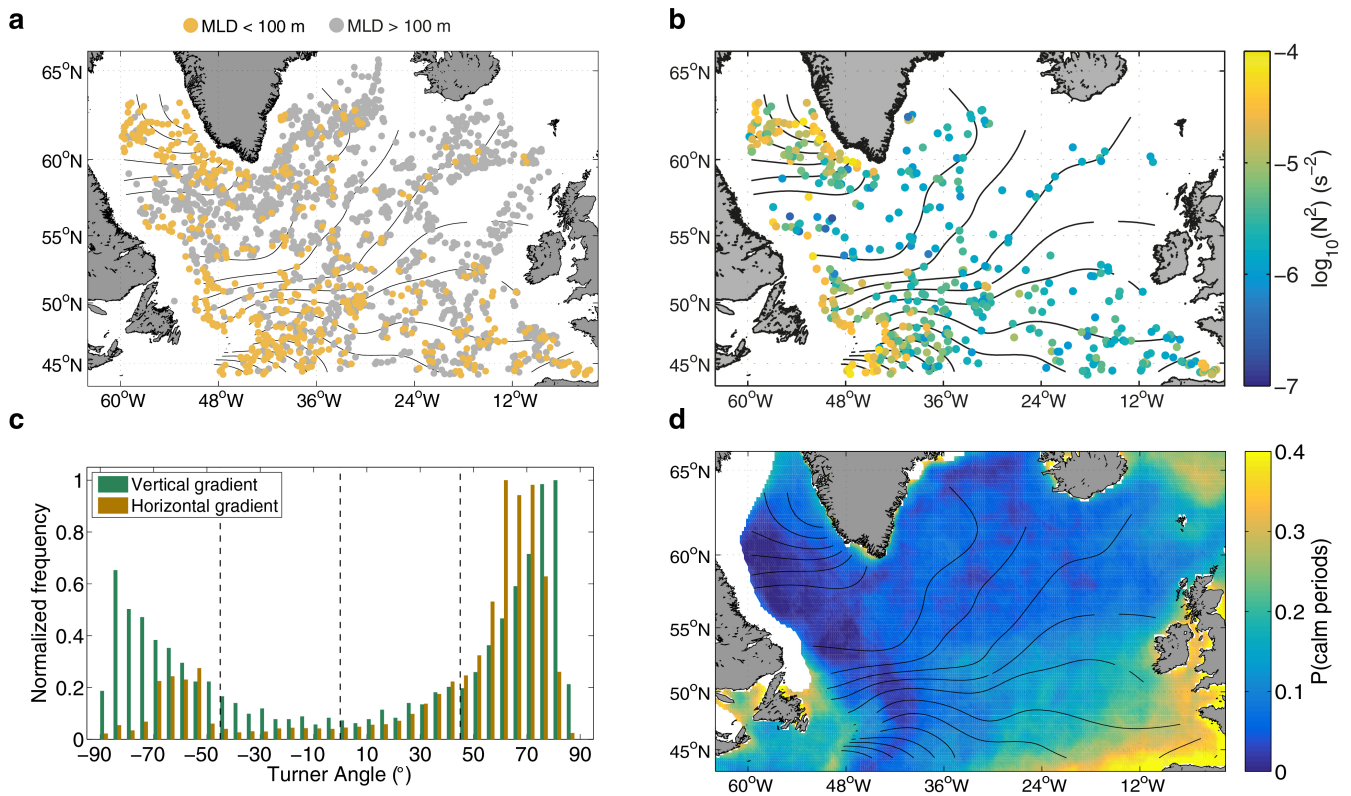
#### 241 **Author contributions**

242 D.I. and L.L. designed the study. L.L., M.A., K.F.S., H.C., A.P., M.R.D. and D.I. conducted  
243 the data analysis. L.L. and M.A. wrote the manuscript. All authors commented on the  
244 manuscript.

245

#### 246 **Competing financial interests**

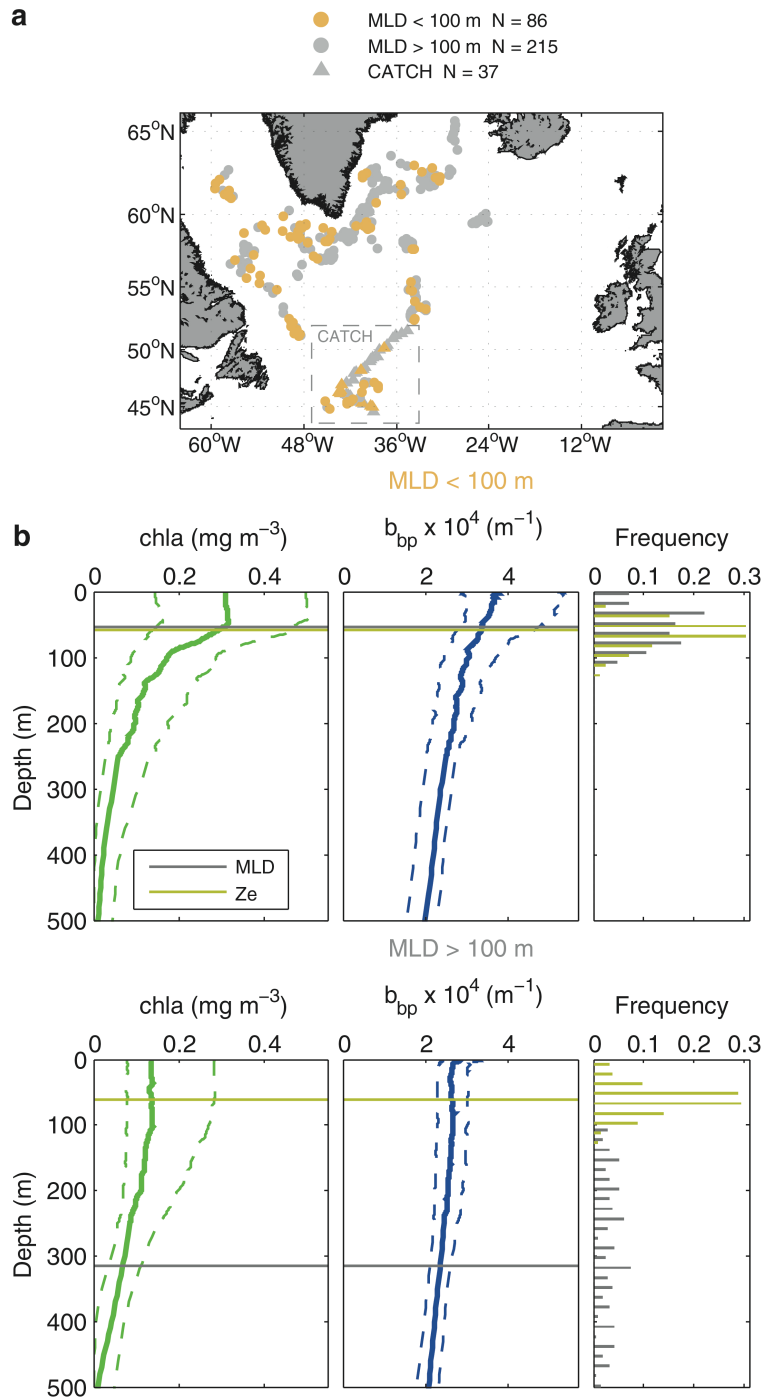
247 The authors declare no competing financial interests.



248

249 **Fig. 1.** Winter mixing intermittency in the North Atlantic Subpolar Gyre. (a) 2022 Argo float  
 250 profiles (January-March 2014-2015). Orange dots mark the location of stratified profiles (MLD  
 251 < 100 m) and grey dots mark the deep mixed profiles (MLD > 100 m). (b) Stratification  
 252 intensity (average value of  $N^2$  between 5 and 100 m) of profiles with MLD < 100 m. (c)  
 253 Frequency distribution of Turner angle for horizontal (orange) and vertical (green) density  
 254 gradients. Each distribution is normalized by its maximum frequency. Vertical dashed lines  
 255 mark angle  $0^\circ$ , where both temperature and salinity contribute equally to the density gradient,  
 256 and angle  $-45^\circ$  and  $45^\circ$  where salinity and temperature respectively are the only contributor.  
 257 Angles  $> 45^\circ$  or  $< -45^\circ$  indicate that salinity is working against temperature and vice versa. (d)  
 258 Probability to have calm periods lasting at least 24 hours during January-March 2014-2015. A  
 259 calm period is defined as a > 24 hour period with wind speed  $< 10 \text{ m s}^{-1}$  and net heat flux  $> -$   
 260  $100 \text{ W m}^{-2}$ . White pixels indicate the presence of sea ice (Supplementary Methods 1.2). Black

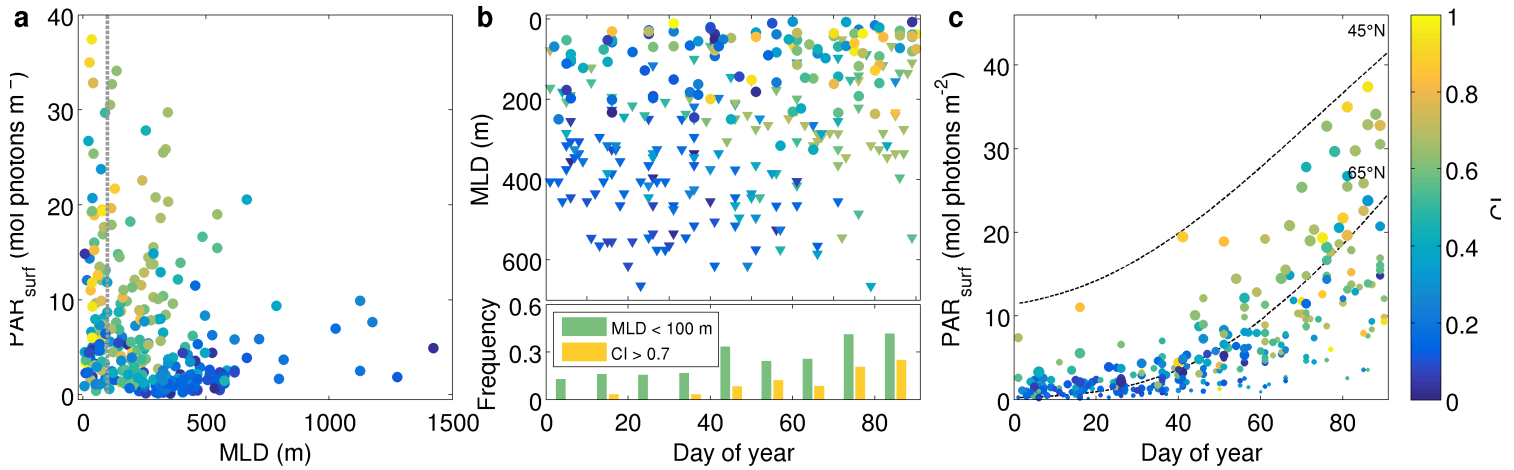
261 lines in (a), (b) and (d) denote contours of surface density (contour interval of  $0.1 \text{ kg m}^{-3}$ ,  
262 maximum and minimum density of  $27.74$  and  $25.90 \text{ kg m}^{-3}$  respectively).



263

264 **Fig. 2.** Winter phytoplankton blooms in the North Atlantic Subpolar Gyre. (a) Location of the  
 265 301 BGC-Argo float profiles (dots, January-March 2014-2015) and the 37 pigment profiles  
 266 from the CATCH cruise (triangles, January-February 1997). Orange symbols indicate stratified  
 267 profiles (MLD < 100 m, 35% of the profiles, including CATCH profiles) and grey symbols  
 268 indicate deep mixed profiles (MLD > 100 m). The dashed rectangle delineates the study area

269 for the CATCH expedition. **(b)** Median profile and quartiles of chlorophyll *a* (chl<sub>a</sub>) and  
270 backscattering (b<sub>bp</sub>) from BGC-Argo floats shown in (a), for MLD < 100 m (top) and MLD >  
271 100 m (bottom). The two sets of data (MLD < 100 m and MLD > 100 m) are statistically  
272 different in term of both surface chl<sub>a</sub> and b<sub>bp</sub> (Wilcoxon test, p-value < 0.01). Every single chl<sub>a</sub>  
273 and b<sub>bp</sub> profile is shown in Supplementary Fig. 9. Horizontal grey and yellow lines indicate the  
274 median MLD and euphotic depth (Z<sub>e</sub>) respectively. Z<sub>e</sub> is defined as the depth of the 0.1 mol  
275 photons m<sup>-2</sup> daily isolume (Supplementary Methods 1.8). Panels on the right show the  
276 frequency distribution of MLD (grey) and euphotic depth (yellow).



277

278 **Fig. 3.** The light environment impacts the phytoplankton community structure. Colour scale  
 279 denotes the optical community index CI (normalized chlorophyll *a* to backscattering ratio). CI  
 280 close to 1 indicates a large contribution of diatoms to the community whereas CI close to 0  
 281 indicates a pico- and nanophytoplankton-dominated community (Supplementary Methods 1.9).  
 282 (a) Surface daily-integrated photosynthetically available radiation (PAR) and MLD derived  
 283 from all BGC-Argo float profiles shown in Fig. 2a. Vertical dashed grey line marks 100 m  
 284 depth. (b) MLD as function of day of year (from 1<sup>st</sup> January to 31 March, top). Circles and  
 285 triangles represent positive and negative MLD anomalies respectively (i.e. deviation from the  
 286 climatological seasonal cycle, supplementary Methods 2.2). Frequency of stratified profiles  
 287 (MLD < 100 m) and frequency of profiles with CI > 0.7 over a ten days period (bottom). (c)  
 288 Surface daily-integrated PAR as function of day of year. Dot size denotes the cloudiness (large  
 289 for clear sky and small for dark sky). Dashed black lines indicate temporal evolution of  
 290 modelled clear sky surface PAR for the minimum and maximum latitudes of the domain (45°N  
 291 and 65°N).